Differential thermopower of a CNT chiral carbon nanotube

2001 J. Phys.: Condens. Matter 13 5653

(http://iopscience.iop.org/0953-8984/13/24/310)

INSTITUTE OF PHYSICS PUBLISHING JOURNAL OF PHYSICS: CONDENSED MATTER

J. Phys.: Condens. Matter **13** (2001) 5653–5662 www.iop.org/Journals/cm PII: S0953-8984(01)18282-2

Differential thermopower of a CNT chiral carbon nanotube

S Y Mensah[1,2], F K A Allotey[2,3], N G Mensah[4] and G Nkrumah[5]

[1] Department of Physics, Laser and Fibre Optics Centre, University of Cape Coast, Ghana
[2] The Abdus Salam International Centre for Theroetical Physics, Trieste, Italy
[3] National Centre for Mathematical Sciences, Ghana Atomic Energy Commission, Kwabenya, Accra, Ghana
[4] Department of Mathematics, University of Cape Coast, Cape Coast, Ghana
[5] Department of Physics, University of Ghana, Legon Accra, Ghana

Received 24 September 2000, in final form 11 April 2001

Abstract

The differential thermopower of a chiral carbon nanotube (CNT) was calculated using a tractable analytical approach. We obtained an expression for the electrical conductivity σ and the thermopower α. The results were numerically analysed. We noted from the values of α that the material can behave as a semimetal, n-type semiconductor and a p-type semiconductor, depending on the parameters of the CNT. We propose the use of the CNT as a thermoelement.

1. Introduction

Carbon nanotubes (CNTs) belong to the family of carbon-based structures formed by wrapping graphite sheets into tube-shaped objects. Each CNT is characterized by a chiral index (m, n), with m and n being two integers which specify it uniquely. This material has recently received a very big boost [1–3]. This is due to the fact that, depending on the method of gluing, a set of atomic carbon structures with a wide spectrum of conducting properties is obtained. They range from insulating, semimetallic or metallic behaviour to semiconductors with a gap of 0–2 eV [4–7]. The unique conducting and capillary properties of the tubulenes make them promising materials for nanoelectronic devices.

Furthermore, there have been many suggestions to use the material as tips for scanning microscopy, ultrastrong mechanical fibre pinning sites for high-T_c superconductors and inclusions in composites for body armour [8]. It is also noted that the CNT is an ideal material to make field emitters because of its usually high aspect ratio as well as its mechanical and chemical stability. Many experiments with single-walled CNTs (SWNTs) [9] and multi-walled CNTs [10, 11] have demonstrated a relatively low threshold voltage of electron emission with little sample degradation [12].

The electronic properties of SWNTs have recently drawn considerable attention. In [13], Kim *et al* studied the electronic density of states (DOS) of a SWNT and characterized sharp Van Hove singularities (VHS) in the DOS using scanning tunneling microscopy (STM) and

compared their data to tight binding calculations for specific tube indices. In [14], a quantum-mechanical treatment of charge-carrier motion in the presence of an external magnetic field was developed. Electron–photon interaction in CNTs has also been studied theoretically by Romanov [15], Kibis and Romanov [16], Chico *et al* [17] and Langer *et al* [18]. In [19] Woods and Mahan studied the electron–phonon effects in graphene and an armchair (10,10) SWNT.

As stated in [20], two broad theoretical approaches for electron transport in nanotubes have emerged. The first approach comprises first principle numerical simulations as exemplified by Miyamoto *et al* [22]. The other approach requires the creation of phenomenological models that yield somewhat rough, but analytically tractable, results [20, 21]. The justification for the latter approach can be established from the work of Miyamoto *et al* [22], where they computed the current excited in carbon and BC_2N nanotubes immersed in an electrostatic field. In that work they established that the current chiral angle (CCA) γ, which is equal to $\tan^{-1}(j_z/j_c)$ (where j_z is the current parallel to the tubular axis, i.e. z-axis and j_c is the circumferential current), can be defined. Moreover, first principle calculation indicated that the CCA is not equal to $\pi/2$ and nor is it equal to the geometric chiral angle (GCA), even though the surface conductivity of the monatomic curved surface of the CNT was taken to be isotropic. Kasumov *et al* [23] and Langer *et al* [18] measured the resistance of a SWNT, their data being in qualitative agreement with theoretical results. Most importantly, the two experimental reports established the validity of the theoretical models.

Thermoelectric properties have been studied in many materials over the past 40 years with the understanding of determining a very good material for thermo devices. Unfortunately, these efforts have met with limited success owing to an accompanying degradation in electrical properties [24]. Relatively recently, attention has been refocused, owing to the appearance of new materials such as the multiquantum wells and superlattices [25]. Superlattices of semiconductors and semimetals are expensive for mass production, even though they show enhancement in the thermoelectric figure of merit Z; hence the need to search for new materials.

In this paper we study the differential thermopower of the chiral CNT. We use the approach in [25] together with the model developed in [20, 21] to determine the thermopower α of the CNT. We observe that the thermopower strongly depends on the GCA θ_h, electric field E, temperature T, the real overlapping integrals for jumps along the tubular axis Δ_z and the base helix Δ_s. The manipulation of these parameters can give rise to high thermopower values, which in our opinion is highly recommendable.

This paper is organized as follows: in section 2 we establish the theory and solution of the problem, and in section 3 we discuss the results and draw conclusions.

2. Theory

We proceed as in [20, 21] by considering an infinitely long chain of carbon atoms wrapped along a base helix as a model of a SWNT. The chief merit of this model is its analytical tractability, which readily yields physically interpretable results. Second, the model yields correct qualitative descriptions of various electronic processes, which are corroborated by first-principle numerical simulations.

The problem is considered in the semiclassical approach by commencing with the Boltzmann kinetic equation [25]:

$$\frac{\partial f(r,\,p,\,t)}{\partial t} + v(p)\frac{\partial f(r,\,p,\,t)}{\partial r} + eE\frac{\partial f(r,\,p,\,t)}{\partial p} = -\frac{f(r,\,p,\,t) - f_o(p)}{\tau}. \qquad (1)$$

Here $f(r,\,p,\,t)$ is the distribution function, $f_o(p)$ is the equilibrium distribution function, $v(p)$ is the electron velocity, E is the constant applied electric field, r is the electron position, p

is the electron dynamical momentum, τ is the electron relaxation time and e is the electron charge.

The collision integral is taken in the τ approximation and further assumed constant. The exact solution of (1) presents some difficulties. We therefore solved it using a perturbation approach with the second term treated as the perturbation. In the linear approximation of ∇T and $\nabla\mu$, we obtain

$$f(p) = \tau^{-1}\int_0^\infty \exp\left(-\frac{t}{\tau}\right) f_o(p - eEt)\,\mathrm{d}t + \int_0^\infty \exp\left(-\frac{t}{\tau}\right)\mathrm{d}t \times\left([\varepsilon(p - eEt) - \mu]\frac{\nabla T}{T} + \nabla\mu\right) v(p - eEt)\frac{\partial f_o(p - eEt)}{\partial\varepsilon} \tag{2}$$

where $\varepsilon(p)$ is the energy of the electron and μ is the chemical potential. The current density is defined as

$$\boldsymbol{j} = e\sum_p \boldsymbol{v}(p) f(p). \tag{3}$$

Substituting equation (2) into (3) and making the transformation

$$p - eEt \to p$$

we obtain for the current density

$$\boldsymbol{j} = e\tau^{-1}\int_0^\infty \exp\left(-\frac{t}{\tau}\right)\mathrm{d}t \sum_p \boldsymbol{v}(p - eEt) f_o(p) + e\int_0^\infty \exp\left(-\frac{t}{\tau}\right)\mathrm{d}t \sum_P \left([\varepsilon(p) - \mu]\frac{\nabla T}{T} + \nabla\mu\right) \times\left(\boldsymbol{v}(p)\frac{\partial f_o(p)}{\partial\varepsilon}\right)\cdot \boldsymbol{v}(p - eEt). \tag{4}$$

Now let us resolve the current along the tubular axis (z-axis) and the base helix, respectively neglecting the interference between the axial and the helical paths connecting a pair of atoms, so that transverse motion quantization is ignored. We then perform the following transformation:

$$\sum_p \to \frac{2}{(2\pi\hbar)^2}\int\int \mathrm{d}p_s\,\mathrm{d}p_z$$

and obtained the electron current density along the tubular axis and the base helix as

$$Z' = \frac{2e^2\tau^{-1}}{(2\pi\hbar)^2}\int_0^\infty \exp\left(-\frac{t}{\tau}\right)\mathrm{d}t\int\int v_z(p_z - eE_z t) f_o(p)\,\mathrm{d}p_s\,\mathrm{d}p_z + \frac{2e^2}{(2\pi\hbar)^2}\int_0^\infty \exp\left(-\frac{t}{\tau}\right)\mathrm{d}t\int\int \left([\varepsilon(p) - \mu]\frac{\nabla_z T}{T} + \nabla_z\mu\right) \times\left(v_z(p_z)\frac{\partial f_o(p)}{\partial\varepsilon}\right) v_z(p_z - eE_z t)\,\mathrm{d}p_s\,\mathrm{d}p_z \tag{5}$$

and

$$S' = \frac{2e^2\tau^{-1}}{(2\pi\hbar)^2}\int_0^\infty \exp\left(-\frac{t}{\tau}\right)\mathrm{d}t\int\int v_s(p_s - eE_s t) f_o(p)\,\mathrm{d}p_s\,\mathrm{d}p_z + \frac{2e^2}{(2\pi\hbar)^2}\int_0^\infty \exp\left(-\frac{t}{\tau}\right)\mathrm{d}t\int\int \left([\varepsilon(p) - \mu]\frac{\nabla_s T}{T} + \nabla_s\mu\right) \times\left(v_s(p_s)\frac{\partial f_o(p)}{\partial\varepsilon}\right) v_s(p_s - eE_s t)\,\mathrm{d}p_s\,\mathrm{d}p_z \tag{6}$$

where the integrations are carried out over the first Brillouin zone. From these two components, expressions for the axial and circumferential components of the current density emerge as follows:

$$j_z = Z' + S' \sin\theta_h \qquad j_c = S' \cos\theta_h \tag{7}$$

where $\theta_\hbar$ is the GCA.

The energy of the electrons, as expressed in [20], is given as

$$\varepsilon(p) = \varepsilon_o - \Delta_z \cos\frac{p_z d_z}{\hbar} - \Delta_s \cos\frac{p_s d_s}{\hbar} \tag{8}$$

where ε_o is the energy of an outer-shell electron in an isolated carbon atom, Δ_z and Δ_s are the real overlapping integrals for jumps along the respective coordinates, p_z and p_s are the carrier momentum along the tubular axis and the base helix respectively, $\hbar$ is Planck's constant, d_z is the distance between the site n and the site $n + N$ along the tubular axis, and d_s is the distance between the site n and $n + 1$ along the base helix.

To calculate the current density for a non-degenerate electron gas we use the Boltzmann equilibrium distribution function expressed as

$$f_o(p) = C \exp\left\{\frac{\Delta_z \cos(p_z d_z/\hbar) + \Delta_s \cos(p_s d_s/\hbar) + (\mu - \varepsilon_o)}{kT}\right\} \tag{9}$$

where

$$C = \frac{d_z d_s n_o}{2\exp[(\mu - \varepsilon_o/kT)] I_0(\Delta_s/kT) I_0(\Delta_z/kT)}$$

n_o is the surface charge density, $I_n(x)$ is the modified Bessel function of order n and k is Boltzmann's constant.

The components v_z and v_s of the electron velocity $\boldsymbol{v}$ are calculated from equation (8) as

$$v_z(p_z) = \frac{\partial\varepsilon}{\partial p_z} = \frac{\Delta_z d_z}{\hbar} \sin\left(\frac{p_z d_z}{\hbar}\right) \tag{10}$$

and

$$v_s(p_s) = \frac{\Delta_s d_s}{\hbar} \sin\left(\frac{p_s d_s}{\hbar}\right). \tag{11}$$

With the help of equations (5)–(11) and the fact that $E_s = E_z \sin\theta_h$ and $\nabla_s T = \nabla_z T \sin\theta_h$, we obtain for the axial j_z and circumferential j_c currents, after cumbersome calculation, the following expressions:

$$\begin{aligned} j_z = {} & (\sigma_z(E) + \sigma_s(E)\sin^2\theta_h)\nabla_z\left(\frac{\mu}{e} - \phi\right) \\ & - \left\{\sigma_z(E)\frac{k}{e}\left(\frac{\varepsilon_o - \mu}{kT} - \Delta_z^*\frac{I_0(\Delta_z^*)}{I_1(\Delta_z^*)} + 2 - \Delta_s^*\frac{I_1(\Delta_s^*)}{I_0(\Delta_s^*)}\right)\right. \\ & \left. + \sigma_s(E)\frac{k}{e}\sin^2\theta_h\left(\frac{\varepsilon_o - \mu}{kT} - \Delta_s^*\frac{I_0(\Delta_s^*)}{I_1(\Delta_s^*)} + 2 - \Delta_z^*\frac{I_1(\Delta_z^*)}{I_0(\Delta_z^*)}\right)\right\}\nabla_z T \end{aligned} \tag{12}$$

$$\begin{aligned} j_c = {} & (\sigma_s(E)\sin\theta_h\cos\theta_h)\nabla_z\left(\frac{\mu}{e} - \phi\right) \\ & - \sigma_s(E)\frac{k}{e}\sin\theta_h\cos\theta_h\left(\frac{\varepsilon_o - \mu}{kT} - \Delta_s^*\frac{I_0(\Delta_s^*)}{I_1(\Delta_s^*)} + 2 - \Delta_z^*\frac{I_1(\Delta_z^*)}{I_0(\Delta_z^*)}\right)\nabla_z T \end{aligned} \tag{13}$$

where ϕ is the electrostatic potential. From equations (12) and (13) the electrical conductivities are given as

$$\sigma_{zz} = \sigma_z(E) + \sigma_s(E)\sin^2\theta_h \tag{14}$$

$$\sigma_{cz} = \sigma_s(E)\sin\theta_h\cos\theta_h \tag{15}$$

where

$$\sigma_z(e) = \frac{n_o e^2 \Delta_z d_z^2 \tau I_1(\Delta_z^*)}{\hbar^2(1+(\Omega_z\tau)^2) I_0(\Delta_z^*)}$$

$$\sigma_s(e) = \frac{n_o e^2 \Delta_s d_s^2 \tau I_1(\Delta_s^*)}{\hbar^2(1+(\Omega_s\tau)^2) I_0(\Delta_s^*)}$$

$$\Omega_z = \frac{eE_z d_z}{\hbar}$$

$$\Omega_s = \frac{eE_s d_s}{\hbar}$$

$$\Delta_i^* = \frac{\Delta_i}{kT} \qquad i = z,\ s.$$

The differential thermoelectric power α is defined as the ratio

$$\frac{|\nabla((\mu/e)-\phi)|}{|\nabla T|}$$

in an open circuit. Hence, of interest to us is α along the axial and circumferential directions, which are obtained from equations (12) and (13) as

$$\alpha_{zz} = \left[\frac{\sigma_z(E)}{\sigma_z(E)+\sigma_s(E)\sin^2\theta_h}\frac{k}{e}\left\{\frac{\varepsilon_o-\mu}{kT} - \Delta_z^*\frac{I_0(\Delta_z^*)}{I_i(\Delta_z^*)} + 2 - \Delta_s^*\frac{I_1(\Delta_s^*)}{I_0(\Delta_s^*)}\right\}\right.$$
$$\left. + \frac{\sigma_s(E)\sin^2\theta_h}{\sigma_z(E)+\sigma_s(E)\sin^2\theta_h}\frac{k}{e}\left\{\frac{\varepsilon_o-\mu}{kT} - \Delta_s^*\frac{I_0(\Delta_s^*)}{I_i(\Delta_s^*)} + 2 - \Delta_z^*\frac{I_1(\Delta_z^*)}{I_0(\Delta_z^*)}\right\}\right] \tag{16}$$

$$\alpha_{cz} = \frac{k}{e}\left[\frac{\varepsilon_o-\mu}{kT} - \Delta_s^*\frac{I_0(\Delta_s^*)}{I_1(\Delta_s^*)} + 2 - \Delta_z^*\frac{I_1(\Delta_z^*)}{I_0(\Delta_z^*)}\right]. \tag{17}$$

3. Results, discussion and conclusion

In this paper we analysed the differential thermopower of a chiral CNT using the tractable analytical approach developed in [20, 21]. Unlike [20, 21], we included the spatial derivative in Boltzmann's equation and solved this for the distribution function. We calculated the total current in the presence of both an electric field and a temperature gradient. We obtained the electrical conductivity σ and the thermopower α. Our expression for σ coincides with that obtained by [20].

The thermopower α is highly anisotropic, depending on the GCA θ_h, the electric field E, temperature T and the real overlapping integrals for jumps along the respective coordinates Δ_z and Δ_s.

For further understanding of the results, we analysed it numerically. Numerical results for the thermopower dependence of temperature are shown in figure 1(a) for fixed values of Δ_z and differing values of Δ_s (measured in electronvolts). Δ_s is varied from 0.015 eV to 0.31 eV. It is noted that when Δ_s is slightly greater than or equal to Δ_z, i.e. $\Delta_s = 0.015$ eV, 0.018 eV or 0.02 eV, the thermopower α decreases rapidly with an increase in temperature T, and at high temperatures it slowly tends to a lower constant value of α, i.e. hyperbolic in nature. This is as expected for semiconducting tubes which exhibit the behaviour $\alpha \sim 1/T$ [26]. Meanwhile, when Δ_s is greater than Δ_z, i.e. when $\Delta_s = 0.031$ eV, the thermopower increases rapidly, gets to a turning point and then decreases slowly to a constant value. The turning point occurs around 100 K. A similar observation was noted in [27], where the thermopower of a SWNT was measured. It becomes obvious that the material, under these conditions is

behaving as a semimetal. The thermopower data in figure 1(a) are positive over the entire range of temperature, indicating that the contribution from positive (hole) carriers dominates the response.

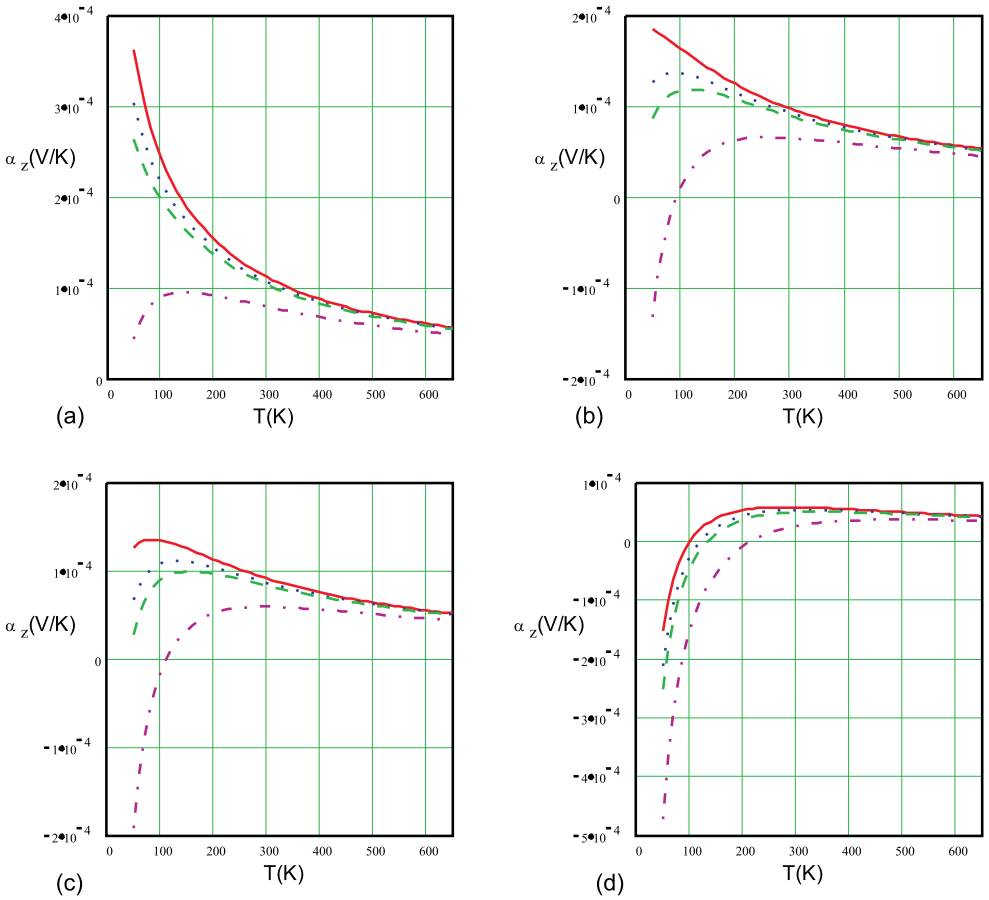

Figure 1. The dependence of thermopower α on temperature T for Δ_s equal to 0.015 eV (——), 0.018 eV (- - - -), 0.020 eV (— —) and 0.031 eV (— – —) for differing values of Δ_z: (a) $\Delta_z = 0.015$ eV, (b) $\Delta_z = 0.024$ eV, (c) $\Delta_z = 0.027$ eV and (d) $\Delta_z = 0.041$ eV.

As Δ_z is increased from 0.015 eV to 0.024 eV, 0.027 eV and 0.041 eV respectively, as can be seen in figures 1(b), 1(c) and 1(d), we observed that most curves indicate turning points at different temperatures, and eventually at $\Delta_z = 0.027$ eV all the curves have turning points. Comparing our results with the experimentally measured α in [28], we note that the theoretical curves agree reasonably well with experiment. We believe that a more sophisticated energy spectrum will be required, but in that case we shall lose the analytical tractability of the problem. What is striking is that the turning points occur in two situations, i.e. when Δ_z is greater than Δ_s and *vice versa*. The turning points shift towards lower temperatures for given Δ_z, but they shift towards greater temperatures as Δ_z increases. One also notes that there exists a threshold temperature for which hole conductivity switches over to electron conductivity, i.e. positive α becomes negative. This can be explained by the fact that graphite has a pair of weakly overlapping electron and hole sp^2 or π bands with near mirror symmetry about the

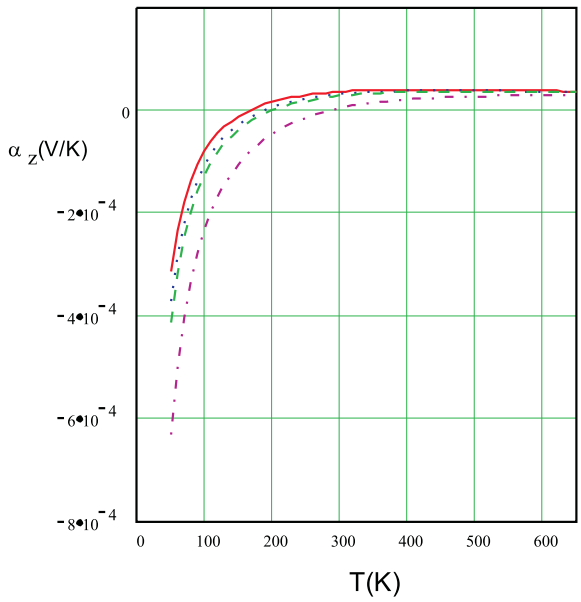

(a)

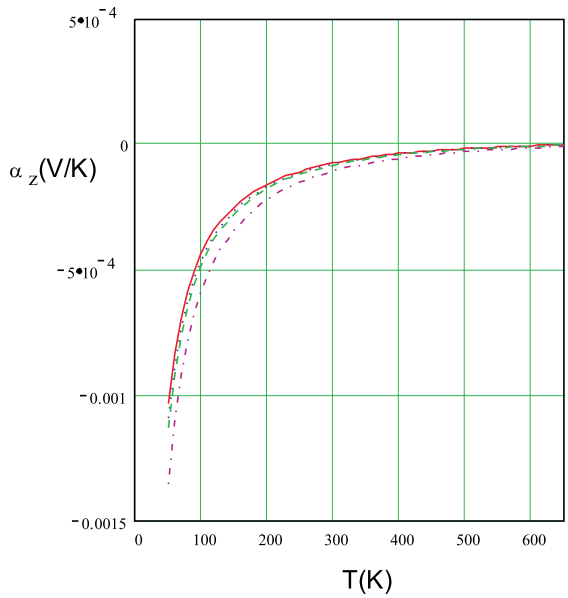

(b)

Figure 2. The dependence of thermopower α on temperature T for Δ_s equal to 0.015 eV (——), 0.018 eV (- - - -), 0.020 eV (— —) and 0.031 eV (— – —) for (a) $\Delta_z = 0.049$ eV and (b) $\Delta_z = 0.085$ eV.

Fermi energy E_F. Approximately equal numbers of electrons and holes in these symmetric π bands are consistent with the negative thermopower observed [28]. The threshold value for the temperature shifts towards lower temperature as we increase Δ_z.

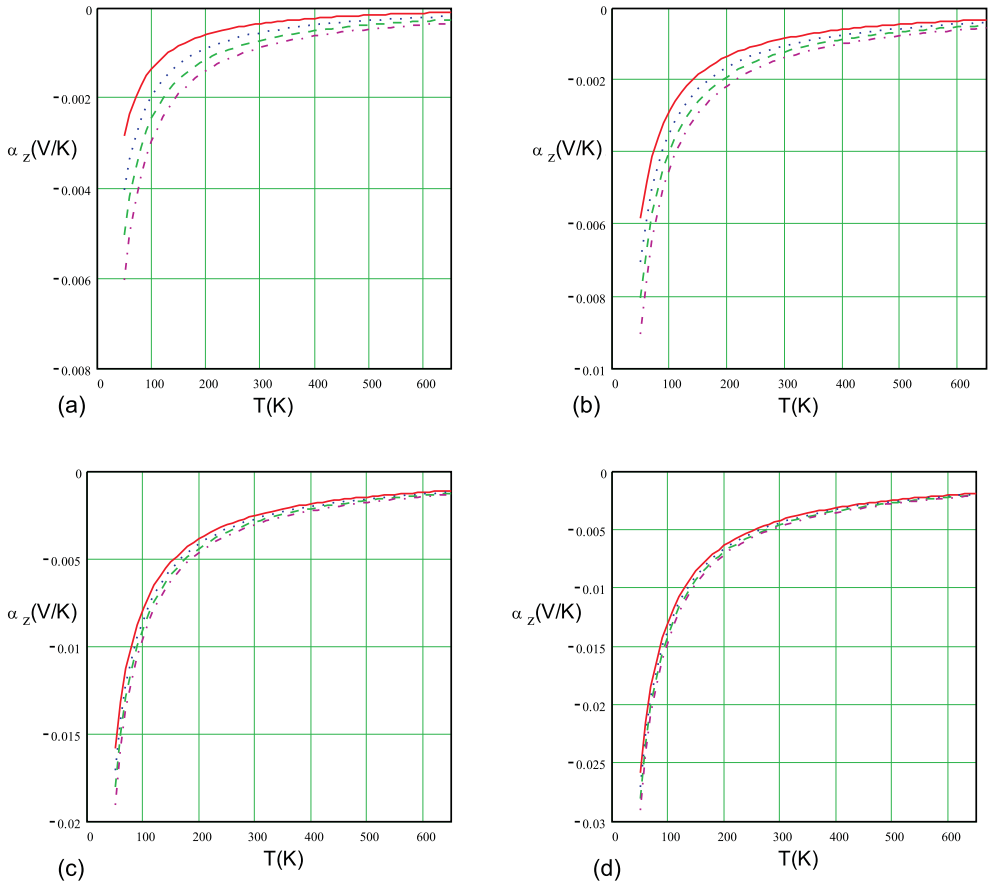

Figure 3. The dependence of thermopower α on temperature T for Δ_s equal to 0.09 eV (——), 0.15 eV (- - - -), 0.20 eV (— —) and 0.25 eV (— – —) for differing values of Δ_z: (a) $\Delta_z = 0.1$ eV, (b) $\Delta_z = 0.25$ eV, (c) $\Delta_z = 0.75$ eV and (d) $\Delta_z = 1.25$ eV.

In figures 2(a) and 2(b) it became clear that for greater values of Δ_z the thermopower α becomes completely n-type and hyperbolic, i.e. $\alpha \sim 1/T$ [26]. We observed in figure 2(b) that at about 600 K onwards, α becomes 0 V K^{-1}. A similar observation was made for armchair symmetry tubes [27]. This was attributed to the mirror symmetry of the coexisting electrons and holes in the overlapping π bands. Finally, we note in figure 3 that as Δ_z increases to 1.25 eV, which corresponds to an undoped CNT, the thermopower becomes completely negative and hyperbolic in nature. This indicates that the material is behaving completely as n-type semiconductor. Kong *et al* [29], in their recent report on SWNT chemical sensors, refer to extrinsic p-type behaviour in their isolated semiconducting SWNT, whilst previously published large positive thermopower data was attributed to intrinsic SWNT behaviour [30].

Finally, we summarized our results with three-dimensional sketches in figure 4. It is worth noting that when $d_s = d_z$ and $\Delta_s = \Delta_z$, as stated in [20], we have a transition from a CNT to a (monolayer) planer graphite sheet as expressed in the isotropic conductivity σ and thermopower α.

It is known that the choice of materials for thermodevices, be they generators, thermocouples or refrigerators, is based on the thermoelectric figure of merit Z defined by

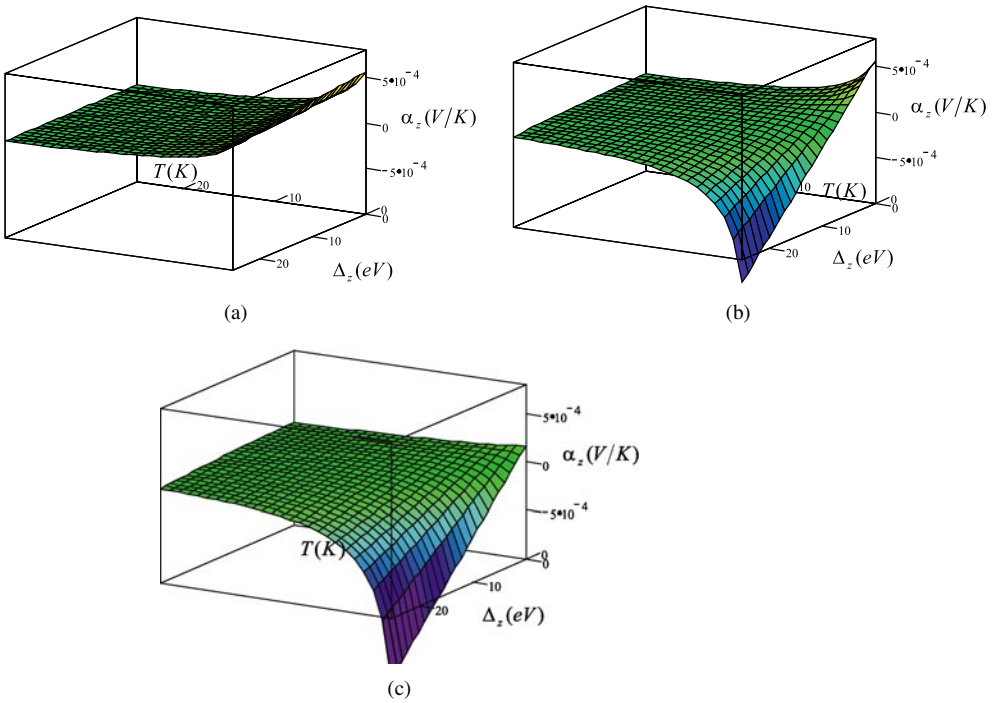

Figure 4. Three-dimensional sketches of $\alpha_z(T, \Delta_z)$: (a) $\Delta_s = 0.01$ eV and 0.01 eV $\leqslant \Delta_z \leqslant 0.02$ eV; (b) $\Delta_s = 0.01$ eV and 0.01 eV $\leqslant \Delta_z \leqslant 0.1$ eV; (c) $\Delta_s = 0.03$ eV and 0.01 eV $\leqslant \Delta_z \leqslant 0.1$ eV. In (a), 1 unit 4.0×10^{-4} eV on the Δ_z axis and 1 unit 24 K on the T axis. In (b) and (c), 1 unit 3.6×10^{-2} eV on the Δ_z axis and 1 unit 24 K on the T axis.

the relation

$$Z = \frac{\alpha^2 \sigma}{\chi}$$

where χ is the thermal conductivity. In our opinion the electrical power factor $\alpha^2\sigma$ involved in Z can be enhanced drastically in CNT by optimizing the choice of the T, Δ_s, Δ_z and θ_h as indicated in the results.

In conclusion, the differential thermopower of a chiral CNT has been investigated theoretically. An excellent analytical expression has been found for σ and α. The determination of α can be used to determine whether the CNT is a semimetal or a semiconductor. Again, the cost in production of CNTs, we hope is cheaper and less sophisticated than a superlattice, and, hence, can be a good material for use as a thermoelement.

Acknowledgments

This work was performed within the framework of the Associateship scheme of the Abdus Salam International Centre for Theoretical Physics, Trieste, Italy. Financial support from the Swedish International Development Cooperation Agency is acknowledged. We also wish to acknowledge C K W Adu for useful discussions.

References

[1] Ebbeson T 1996 *Phys. Today* **49** 26
[2] Ijima S 1991 *Nature* **54** 56
[3] Rodriguez N M 1993 *J. Mater. Res.* **8** 3233
[4] Mintmire J W, Dunlap B I and White C T 1992 *Phys. Rev. Lett.* **68** 631
[5] Saito R, Fujita M, Dresselhaus G and Dresselhaus M S 1992 *Appl. Phys. Lett.* **60** 2204
[6] Hamada N, Sawada S and Oshiyama A 1992 *Phys. Rev. Lett.* **68** 1579
[7] Mintmire J W, Robertson D H and White C T 1993 *J. Chem. Phys. Solids* **54** 1835
[8] Kane C, Balents L and Fisher M P A 1997 *Phys. Rev. Lett.* **79** 5086
[9] Bonard J M, Salvetat J P, Stockli T and de Heer W A 1998 *Appl. Phys. Lett.* **73** 918
[10] Wang Q H, Corrigan T D, Dai T Y and Chang R P H 1997 *Appl. Phys. Lett.* **70** 3308
[11] de Heer W A, Chatelain A and Ugarte D 1995 *Science* **270** 1179
[12] Han S and Ihm J 2000 *Phys. Rev.* B **61** 9986
[13] Kim P, Odom T W, Huang J L and Lieber C M 1999 *Phys. Rev. Lett.* **82** 1225
[14] Kibis O V 1992 *Fiz. Tverd. Tela* **34** 3511 (Engl. transl. 1992 *Sov. Phys. Solid State* **34** 1880)
[15] Romanov D A 1992 *Pis Zh. Eksp. Teor. Fiz.* **55** 703 (Engl. transl. 1992 *JETP Lett.* **55** 738)
[16] Kibis O V and Romanov D A 1995 *Fiz. Tverd. Tela* **37** 127 (Engl. transl. 1995 *Phys. Solid State* **37** 69)
[17] Chico L, Crespi V H, Benedict L X, Louie S G and Cohen M L 1996 *Phys. Rev. Lett.* **76** 971
[18] Langer L, Bayot V, Grivei E, Issi J P, Heremans J P, Oik C H, Stockman L, Van Haesendonck C and Bruynseraede Y 1996 *Phys. Rev. Lett.* **76** 479
[19] Woods L M and Mahan G D 2000 *Phys. Rev.* B **61** 10 651
[20] Slepyan G Ya, Maksimenko S A, Lakhtakia A, Yavtushenko O M and Gusakov A V 1998 *Phys. Rev.* B **57** 9485
[21] Yavtushenko O M, Slepyan G Ya, Maksimenko S A, Lakhtakia A and Romanov D A 1997 *Phys. Rev. Lett.* **79** 1102
[22] Miyamoto Y, Louie S G and Cohen M L 1996 *Phys. Rev. Lett.* **76** 2121
[23] Kasumov A Yu, Khodos I I, Ajayan P M and Colliex C 1996 *Europhys. Lett.* **34** 429
[24] Rowe R D, Hin G and Kuznestsov V L 1998 *Phil. Mag.* **77** 105
[25] Mensah S Y and Kangah G K 1992 *J. Phys.: Condens. Matter* **4** 919
[26] Sumanasekera G U, Adu C K W, Fang S and Eklund P C 2000 *Phys. Rev. Lett.* **85** 1096
[27] Hone J, Ellwood I, Muno M, Mizel A, Cohen M L and Zettl A 1998 *Phys. Rev. Lett.* **80** 1042
[28] Grigorian L, Sumanasekara G U, Loper A L, Fang S L, Allen J L and Eklund P C 1999 *Phys. Rev.* B **60** R309
[29] Kong *et al* 2000 *Science* **275** 622
[30] Grigorian L *et al* 1998 *Phys. Rev. Lett.* **80** 5560